Fire Behaviour of GFRP-Reinforced Concrete Slab Strips: Fire Resistance Tests and Numerical Simulation

António P. C. Duarte, Inês C. Rosa, Mário R. T. Arruda, João P. Firmo[✉],
and João R. Correia

CERIS, Instituto Superior Técnico, Universidade de Lisboa, Lisbon, Portugal
`joao.firmo@tecnico.ulisboa.pt`

Abstract. This paper presents experimental and numerical investigations on the fire behaviour of GFRP-reinforced concrete (RC) slab strips. In the first part of this study fire resistance tests were performed on four concrete slab strips reinforced with sand-coated GFRP bars, in which the influence of the following parameters was assessed: (i) the concrete cover thickness; (ii) the presence of cold anchorages in the GFRP rebars, (iii) the presence of lap splices in the fire-exposed length and (iv) the concrete strength. The specimens were tested in a four-point bending configuration, being subjected to a sustained service load, while the bottom surface was exposed to the ISO 834 fire curve. These experiments were then complemented with the development of three dimensional (3D) thermo-mechanical finite element (FE) models of the slab strips to simulate the fire resistance tests. Both the temperature-dependent thermo-physical and mechanical properties of the constituent materials were considered; the GFRP-concrete interaction was also modelled by means of local bond *vs.* slip laws, which were previously calibrated by the authors for different temperatures. Comparisons between numerical and experimental results confirmed the accuracy of the FE models in predicting the thermo-mechanical response of GFRP-RC slab strips during fire exposure, namely in terms of temperatures, midspan deflection increase with time, failure modes and fire resistance. Both experimental and numerical results confirmed that (i) the fire resistance can be drastically reduced when the rebar splices are directly exposed to heat, and (ii) even adopting relatively small concrete cover thicknesses it is possible to attain considerable fire endurances provided that the anchors of the GFRP rebars remain sufficiently cold. Moreover, the specimen manufactured with a higher concrete strength presented less extensive cracking, reducing the localized heating of the reinforcement and leading to a higher fire resistance.

Keywords: GFRP-reinforced concrete · Fire resistance tests · FE modelling · GFRP-concrete bond

1 Introduction

In spite of their higher initial costs, fibre reinforced polymer (FRP) bars are being increasingly used as internal reinforcement of concrete structural elements owing to their several

advantages over conventional steel rebars: high strength, lightness and, more importantly, high corrosion resistance. However, there are several uncertainties and well-founded concerns about their fire performance, since both the mechanical and bond properties of FRP rebars experience significant reductions, especially when approaching the glass transition temperature (T_g) of the polymeric matrix (usually between 65–150 ºC). Despite the susceptibility of FRP reinforcement to elevated temperatures and its inherent influence on the fire performance of RC structures, previous research has proven that FRP-reinforced concrete (RC) members can attain significant fire endurances, in some cases well above 90 min (e.g. Nigro et al. 2012 and Hajiloo et al. 2019). Guaranteeing cold anchorage zones at the extremities of the rebars (*i.e.*, maintaining their temperature below T_g), where the bond to concrete remains largely unaffected during fire exposure, has been proven key for such performance. With such proper insulation at the ends of the FRP reinforcement, failure is likely to occur due to the tensile failure along the heated span for considerably higher temperatures than those causing the loss of bond. However, in real structural members, especially when rebar splicing is needed, bond failures in those regions can trigger premature collapses during fire exposure. In fact, the limited research carried out so far (*e.g.* Carvelli et al. 2013) has identified this detail as critical to the fire endurance of lap-spliced FRP-RC members, especially if located in spans directly exposed to heat, as the loss of bond in the splices occurs at relatively low temperatures (around the T_g).

One of the main parameters that governs the fire resistance of FRP-RC members is the concrete cover thickness; in most previous investigations (*e.g.* Nigro et al. 2011, 2012 and Hajiloo et al. 2019) the influence of this parameter was assessed in members with relatively high concrete cover thicknesses (between 32 and 60 mm); from a durability point of view this does not represent an efficient use of FRP materials, since in real applications the corrosion resistance of composite rebars allows adopting lower concrete cover thicknesses. The very few studies available comprising members with low (and more realistic) concrete cover thicknesses (*e.g.* Kodur and Bisby 2005; Kodur et al. 2005) assessed the thermal response of FRP-RC specimens exposed to fire without any structural loading.

The numerical simulation of the thermo-mechanical response of FRP-RC structures during fire has been assessed in a limited number of studies (Nigro et al. 2011; Kodur and Bisby 2005; Adelzadeh et al. 2014; Rafi and Nadjai 2014), and most of them have empirically predicted the fire resistance of structural members based on critical temperatures in FRP instead of simulating their actual mechanical response (and failure modes). In these numerical studies a perfect FRP-concrete interaction has been assumed owing to insufficient information about the temperature dependency of the FRP-concrete bond laws – although this simplification is acceptable when bond failures are not expected (*i.e.*, when the FRP anchor zones remain cold during fire exposure), to accurately simulate/predict the premature collapse that may occur in lap-spliced members, the FRP-concrete bond degradation with temperature has to be considered.

Despite the relevance and the concerns about the fire behaviour of FRP-RC structures, this topic has not yet been fully addressed in the literature and this has been hampering the use of FRP reinforcement in structures where the fire action have to be considered in design. In fact, as a consequence of these knowledge gaps, the main design

guidelines still discourage the use of FRP rebars in constructions likely to be exposed to fire (*e.g.* buildings) and/or recommend very high (conservative and uneconomical) values of concrete cover.

The current paper presents further experimental and numerical investigations on the behaviour of FRP-RC slabs exposed to fire in order to provide a better understanding about this topic, namely regarding the effects of (i) cold anchorages, (ii) lap splices along the span, (iii) concrete strength and (iv) concrete cover - for these aspects, the information available in the literature is either very limited (cold anchorages, concrete strength and cover thickness) or not comprehensive (lap splices). To this end, fire resistance tests were performed in simply supported RC slab strips reinforced with sand-coated glass-FRP (GFRP) bars; the slabs were simultaneously loaded in bending and heated from the bottom according to the ISO 834 standard fire curve. The temperatures were monitored along the span, at the extremities of the longitudinal reinforcement (protected from direct heating) and along the lap splices (intentionally located along the span). This experimental campaign was complemented with the development of three dimensional (3D) thermo-mechanical finite element (FE) models of the slab strips to simulate the fire resistance tests. Both the temperature-dependent thermo-physical and mechanical properties of the constituent materials were considered; the GFRP-concrete interaction was also modelled by means of local bond *vs.* slip laws previously calibrated by the authors (Rosa et al. 2019) for different elevated temperatures.

2   Description of the Fire Resistance Tests

The fire resistance tests were performed on three slab strips with a length of 1.50 m (clear span of 1.40 m), and cross-section width and thickness of 0.25 m and 0.11 m, respectively, as illustrated in Fig. 1. The internal GFRP reinforcement consisted of 10 mm and 6 mm diameter bars, respectively for the lower and upper longitudinal layers; 6 mm diameter rebars was also applied in the transverse direction in both layers. The GFRP rebars with 10 mm and 6 mm in diameter presented ultimate tensile strengths of 896 MPa and 1045 MPa, and elastic modulus of 46 GPa and 48 GPa, respectively (average values obtained from tensile tests according to ISO 10406-1 standard). The glass transition temperature (T_g) of the rebars was 98 ºC, determined based on the onset of the storage modulus curve decay, obtained through dynamic mechanical analyses (DMA). The decomposition temperature ($T_d = 380$ ºC) was obtained from differential scanning calorimetry (DSC) and thermogravimetric analyses (TGA) based on the middle temperature of the sigmoidal mass change.

The slab strips were produced using ready-mixed concrete (limestone aggregates and Portland cement type CEM II/A-L 42.5 R). Two concrete mixes were used with a lower (mix 1) and higher (mix 2) strength, presenting the following average properties at the age of testing (643 and 135 days, respectively): cube compressive strengths of 35.1 MPa and 53.3 MPa; splitting tensile strengths of 2.0 MPa and 2.8 MPa, respectively for concrete mix 1 and 2.

The four slab strips tested differed in the concrete cover (2.5 cm or 3.5 cm), concrete strength (mix 1 or 2) and in the continuity of the GFRP reinforcement (continuous or lap-spliced). In the slab with lap-spliced reinforcement (named as GFRP-LS65), the overlap

length (65 cm) corresponded to the design development length obtained according to ACI 440.1R-15 design guideline for ambient temperature conditions. In order to trigger failure in the splice, it was intentionally located at midspan and directly exposed to the fire. The main characteristics and nomenclature of the slab strips are summarized in Table 1.
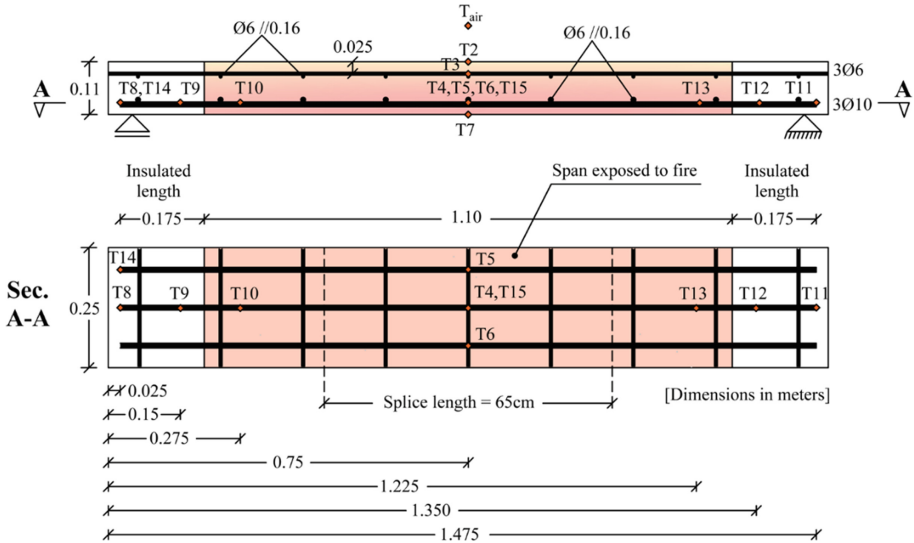

Fig. 1. Geometry of the slab strips and position of the thermocouples: longitudinal view (top) and cross-section view (bottom).

Table 1. Details of the slab strips tested.

Slab strip	Concrete cover [cm]	Concrete mix	Bar continuity	Fire load [kN]
GFRP-C2.5	2.5	1	Continuous	16.9
GFRP-C3.5	3.5	1	Continuous	13.6
GFRP-C3.5*	3.5	2	Continuous	13.6
GFRP-LS65	2.5	1	Spliced (65 cm overlap length)	16.9

The fire resistance tests were performed in an intermediate scale furnace using the test setup depicted in Fig. 2. The bottom surface of the slabs was exposed to the ISO 834 standard fire over a length of 1.10 m, whereas their lateral sides were thermally insulated. The anchorage zones of the longitudinal reinforcement were thus protected from direct fire exposure in each end of the slabs over a length of 0.175 m (*cf.* Fig. 1). The slab strips were loaded in a four-point bending simply supported configuration, consisting of two concentrated loads applied at thirds of the 1.40 m span, corresponding to 70% of

the design load at ambient temperature, set according to Eurocode 2 part 1–1 (*cf.* Table 1); for the slabs with 2.5 cm of concrete cover, such load level resulted in circa 58% of the failure load obtained in flexural tests previously conducted at ambient temperature, whereas for the slab with 3.5 cm of cover it corresponded to 68% of its flexural strength.

Regarding the instrumentation, the midspan displacement was measured at the top surface of the slabs, while the temperatures were continuously measured in the following locations (denoted by 'T#' in Fig. 1): (i) in the air above the slabs, (ii) in the concrete (at different depths in the midspan section), and (iii) in the longitudinal reinforcement (along the exposed span and in the protected anchorage zones).

The fire resistance tests started with the application of the structural loading by suspending weights through a load transmission beam (*cf.* Fig. 2). After a period of about 30 min, set in order to guarantee the stabilization of deflections, the bottom surface of the slabs was exposed to the ISO 834 standard fire curve until failure. The main experimental results obtained are shown alongside with their numerical counterparts in Sect. 4.
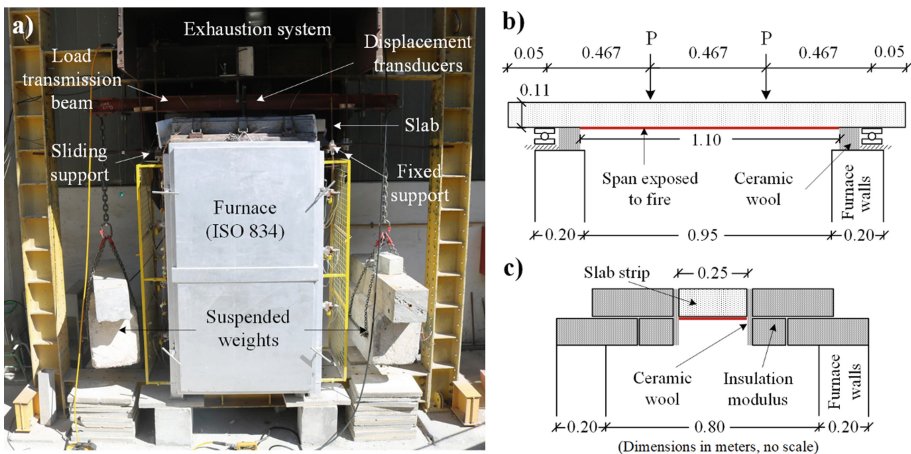

Fig. 2. Fire resistance tests setup: a) general view; b) longitudinal, and c) transversal scheme of the furnace and insulation system.

3 Description of the Numerical Models

Three-dimensional (3D) finite element (FE) models of the slabs strips were developed using the commercial package ABAQUS. In order to simulate the fire resistance tests, two types of analyses were performed: (i) thermal, to simulate the evolution of temperatures in the slabs, and (ii) thermomechanical, to simulate the mechanical response under fire exposure. To reduce the computational effort, only 1/6 (in the case of slab strips with continuous reinforcement) or 1/3 (for the lap-spliced) of the slab strips were modelled - adequate symmetry boundary conditions were used. Figure 3 shows the geometry and mesh of the FE models, which consisted of three parts: concrete slab strip, GFRP reinforcement bars and loading/bearing steel plates, all modelled with 8-node solid finite

elements (C3D8 in ABAQUS designation). The maximum dimension of the FEs in the concrete part along the X-axis was defined as 1/10 of the width of the slab strip, with their length and height along the other directions having the same approximate value (maximum differences of 5%). The length of the FEs (along the Z-axis) in the GFRP bars was chosen in order to match that of the FEs of the concrete part and their cross-sections were discretized with 10 FEs. Finally, the steel plates were discretized with FEs with an average side of circa 12 mm.

The temperature dependence of the properties of all constituent materials was incorporated in the models due its significant influence on the thermal and mechanical responses of the slabs when subjected to fire. Steel was modelled as linear elastic and all properties were defined according Eurocode 3. For concrete, a classical damaged plasticity model was adopted; its mechanical properties at ambient temperature were defined based on the tests performed in the present study, and the variation with temperature of both thermo-physical and mechanical properties of concrete were assumed according to Eurocode 2 (for limestone aggregates); the values of concrete fracture energy were estimated using the equations proposed by Hilsdord and Brameshuber (1991), and were assumed constant with temperature (according to Bamont and Felicetti 2012).
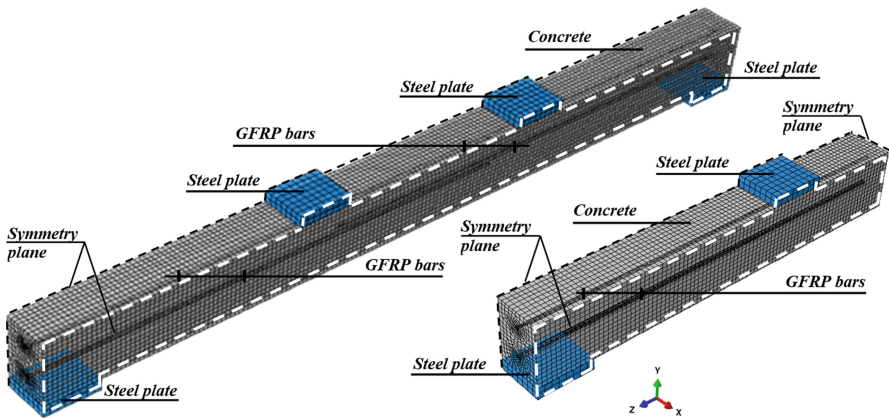

Fig. 3. Geometry and mesh of GFRP-LS65 (left) and GFRP-C3.5 (right) models.

The GFRP rebars were considered as linear elastic and isotropic. Their thermo-physical properties were assumed according to Bai et al. (2007); regarding the mechanical properties (tensile strength and elasticity modulus) as a function of temperature, up to 300 °C they were defined according to the tensile tests previously performed by the authors (Rosa et al. 2019); for higher temperatures, the reductions proposed by Wang et al. (2007) were adopted. For the interaction between GFRP bars and concrete, contact with cohesive surfaces was adopted, which comprised the definition of the stiffness of the contact, and also of the damage initiation and propagation. These bond properties were defined according to the local bond *vs*. slip laws proposed in Rosa et al. (2019) (*cf*. Fig. 4), which were previously and independently calibrated by the authors for different

temperatures based on pull-out tests performed up to 140 ºC; for higher temperatures, the GFRP-concrete interaction was assumed to be negligible.

To simulate the fire behaviour of the slabs, a sequentially uncoupled thermo-mechanical procedure was performed: a heat transfer analysis (with a maximum time step of 50 s) was first performed to obtain the temperature distributions for a similar duration to that of the tests; next, a mechanical analysis was carried out, considering the thermal data determined in the previous step.
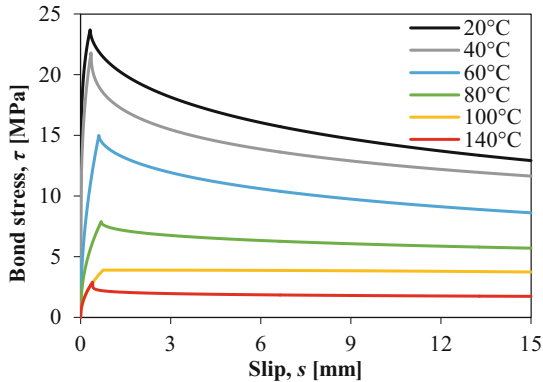

Fig. 4. Local bond *vs.* slip laws used to simulate the GFRP-concrete interaction at different temperatures (Rosa et al. 2019).

4   Results and Discussion

4.1   Temperature Profiles

Figure 5 shows representative temperature profiles measured during the fire resistance tests on slabs GFRP-C2.5 and GFRP-C3.5[1]. The temperatures measured (at midspan) in the slab with lap-spliced reinforcement (GFRP-LS65) were only slightly higher (maximum differences of 30 ºC) than those obtained in slab GFRP C2.5 (with continuous rebars and the same concrete cover thickness), most likely due to more extensive cracking in the former (*cf*. Fig. 7).

As shown in Fig. 5, temperatures measured by the thermocouples located next to the slabs' bottom surface (T7) followed closely the ISO 834 standard fire curve (not plotted); temperatures progressively increased with time in all thermocouples, even if at different rates. As expected, slab GFRP-C3.5 presented lower temperatures in the reinforcement due to the increased thermal protection provided by the thicker layer of concrete cover when compared to slab GFRP-C2.5 (*i.e.* 3.5 *vs.* 2.5 cm). The benefit of the cover increase was not relevant in the anchorage zones, since proper insulation of that region was intentionally provided by the test setup adopted (*cf.* Fig. 7e); however,

---

[1] Temperatures measured in slab GFRP-C3.5* were similar to those in slab GFRP-C3.5.

significant differences were obtained in thermocouples located in the span exposed to fire. In all slabs, when the concrete temperature approached 100 ºC, the heating rates decreased considerably (increasing again a few minutes later) due to the moisture evaporation. It is worth mentioning that no spalling was detected during the tests.

As expected, the temperatures in the bottom reinforcement varied significantly from the directly exposed zones (*cf*. Fig. 1) to the insulated length located over the supports. For example, when slab GFRP 2.5 failed, the average temperature in the reinforcement at midspan section (T4) was around 500 ºC, whereas at the extremities (T8) it was only 30 ºC (below T_g). However, 10 cm away from the latter thermocouples (T9, located in an unexposed zone, but closer to the furnace), the temperature at such instant was 115 ºC. This means that even though the unexposed zone was 20 cm long (on each side), less than half of this distance was below the T_g of the GFRP rebars when the slab failed.

Figure 5 also shows representative temperature distributions obtained from the numerical models, where it can be seen that a general good agreement was obtained; these results show that the FE models were able to reproduce the temperature distribution along the thickness of both slabs. Yet, it is worth mentioning that the heating rate reduction measured in the tests due to moisture evaporation (*e.g.* curves of thermocouples T2 and T4) was not captured by the numerical models, which retrieved a relatively continuous temperature increase for that temperature range. These relative differences should stem from the higher moisture content in the slab strips tested compared to what was considered in the FE models.
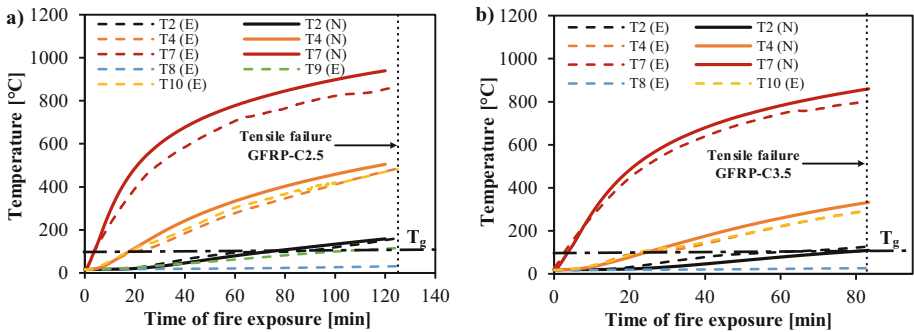

Fig. 5. Representative temperature profiles obtained during fire resistance tests (dashed lines) and from the numerical models (continuous lines): (a) slab GFRP-C2.5; (b) slab GFRP-C3.5.

4.2 Mechanical Behaviour During Fire Exposure

Figure 6(a) presents both experimental and numerical curves in terms of midspan displacement increase *vs.* time of fire exposure. This figure shows that slab GFRP-C3.5 failed after 83 min of fire exposure, that is considerably sooner than slab GFRP-C2.5 (124 min) – the lower fire resistance of slab GFRP-C3.5 may be explained by the development of a wider crack in the heated length of this slab, leading to higher temperatures in the bottom reinforcement (in that cracked section) and, therefore, causing its tensile

failure due to this localized heating. As can be observed in this figure, the curve of slab GFRP-C3.5* was similar to that of slab GFRP-C3.5 (up the failure instant of the latter), but did not exhibit any premature failure – this result can be explained by the less extensive cracking developed in the former slab as consequence of the higher concrete strength used in its production, thus reducing the localized heating of the bottom reinforcement. In this regard, it is worth mentioning that the numerical models developed in this study cannot simulate these local heating phenomena that may have caused the premature failure of slab GFRP-C3.5; for this reason, only the results of the mechanical response of slab GFRP-C3.5* were used for comparison with the predictions obtained from the numerical model, as presented next.
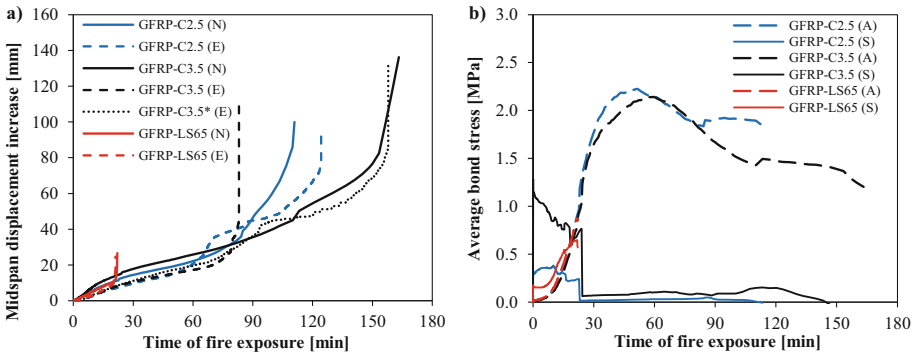

Fig. 6. (a) Experimental (E) and numerical (N) midspan displacement increase *vs.* time of fire exposure curves; (b) average bond stress at the bottom rebars-concrete interface along the central span (*i.e.* heated, labelled as "S") and in the anchorage zones (thermally insulated, labelled as "A").

From a qualitative point of view, the midspan displacement *vs.* time curves of slabs GFRP-C2.5 and GFRP-C3.5* presented the same development stages, though occurring at different time intervals, mainly due to the insulation effect provided by the increased concrete cover in the latter specimen. In the first stage, which took place during the first 60 min for slab GFRP-C2.5 and around 70 min for slab GFRP-C3.5*, the midspan displacement presented a moderate increase at an approximately constant rate. At the end of this stage, the temperatures in the bottom reinforcement at midspan were similar in both slabs, 305 ℃ and 310 ℃ (well above the T_g of the GFRP), respectively, while at the unexposed zones temperatures below T_g were registered. As most of the bond strength of these rebars is lost for temperatures above T_g (*cf.* Rosa et al. 2019), a progressive loss of bond from the heated length of the slabs towards the insulated extremities occurred during this stage, as a consequence, the behaviour of the bottom reinforcement can be compared to that of a "cable", anchored in the cooler extremities of the slabs (which were kept below T_g). In fact, the numerical results presented in Fig. 6(b) show that the development of this "cable" behaviour occurred during an early stage of the tests (before 30 min) – as can be seen in this figure, when the average bond stress at the rebar-concrete interface along the central (*i.e.* heated) length decreased to zero, an instantaneous increase of the

bond stress at the anchorage (*i.e.* insulated) zones occurred, confirming the development of such transfer mechanism.

In the next stage (from 60 to 70 min for slab GFRP-C2.5, and from 70 to 95 min for slab GFRP-C3.5*), the displacement rates increased significantly in both slabs – this behaviour may be partially explained by the higher reduction rate of the tensile modulus of the rebars for temperatures close to T_d (380 ºC). After 70 min and 95 min of fire exposure, respectively in slabs GFRP C2.5 and GFRP C3.5*, the rates of displacement increase reduced considerably, maintaining an approximately constant rate (similar to what was observed in the first stage) up to around 110 min and 135 min of exposure, respectively. During this stage, the temperatures of the bottom rebars in the region directly exposed to fire exceeded the T_d (380 ºC); therefore, the reduction in the displacement rate is partially explained by the further degradation with temperature of the elastic modulus of the rebars, which is significantly less pronounced than the degradation of the GFRP-concrete bond (*cf.* Rosa et al. 2019). The final stage extended until failure of the slabs, which occurred due to tensile rupture of the rebars at midspan (*cf.* next section).

Regarding the effect the lap-spliced reinforcement, as expected, it remarkably reduced the fire endurance to less than 30 min; in slab GFRP-LS65 failure occurred due slippage of the bottom reinforcement after 21 min of fire exposure; at that instant, the rebars' temperature was well above the T_g (146 ºC). It is worth reminding that the development length adopted in this slab corresponded to that provided by the guidelines used for design at ambient temperature; this result confirms that special detailing considerations must be taken into account when designing lap-spliced GFRP-RC elements, namely avoiding splicing along spans susceptible to fire, namely locating them over the supports or in the upper (cool) areas of the cross-section (for thicker cross-sections and if using bent reinforcement).

The numerical curves depicted in Fig. 6(a) present an overall good agreement with their experimental counterparts, either regarding the displacement increase with time or the fire resistance of all slabs (with the exception of slab GFRP-C3.5, due to the premature failure mentioned above). Moreover, the numerical models were also able to predict the failure modes observed in the tests (*cf.* Sect. 4.3): tensile failure of the bottom rebars in the slabs with continuous reinforcement and bond failure in the lap-spliced slab – this agreement further validates the thermo-mechanical FE models and also the local bond-slip laws previously (and independently) calibrated by the authors (in Rosa et al. 2019).

4.3   Failure Modes and Post-fire Observations

Figure 7 shows representative pictures of the slabs after the fire resistance tests; the failure mode obtained in the numerical model of slab GFRP-C2.5 is also shown for illustrative purposes. As expected, the bottom surface of the slabs with continuous reinforcement, which was exposed to very high temperatures for more than 90 min and then cooled down to ambient temperature, exhibited considerable disaggregation of the superficial cement paste (*cf.* Fig. 7c); spalling of the concrete cover was not observed in the tests. Figure 7(a) shows that several main cracks opened between the load application points – the formation of these cracks was also predicted by the FE model (*cf.* Fig. 7(b). After the tests, the concrete cover was removed to confirm the failure mode and to assess the
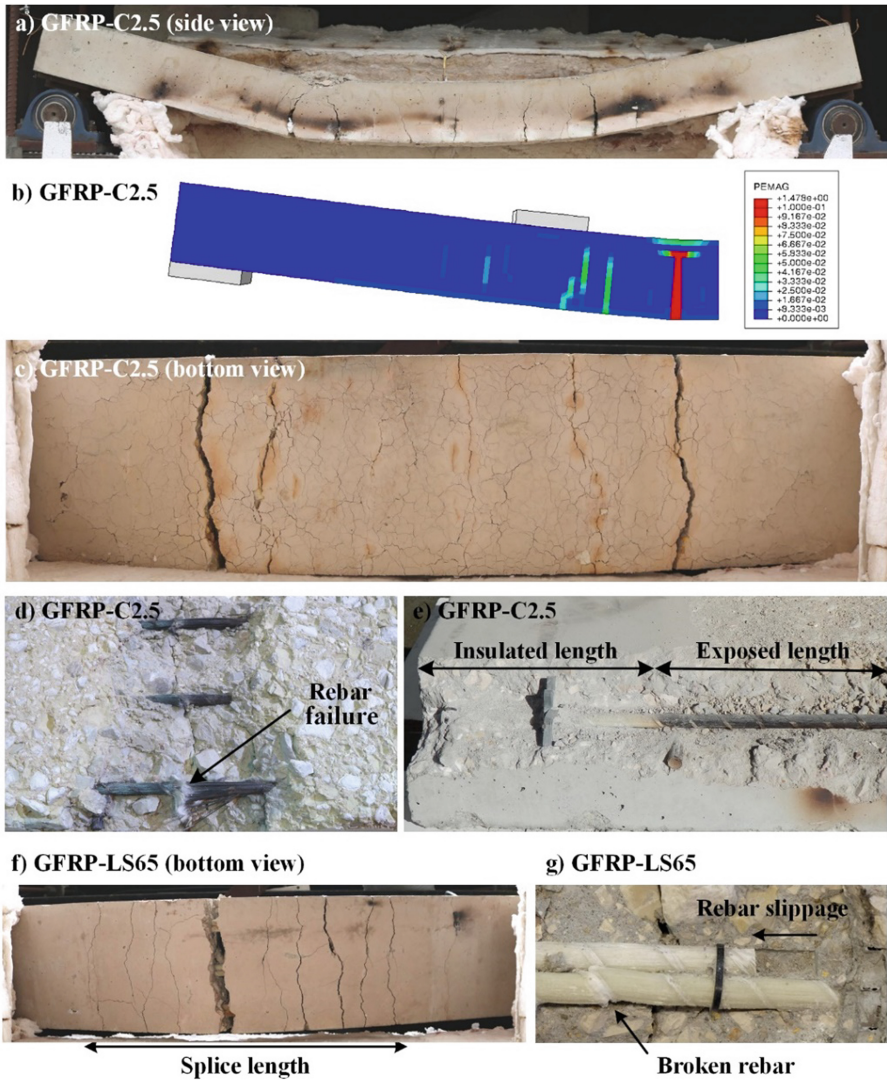
Fig. 7. View of the slabs after the fire resistance tests with continuous reinforcement (a, c, d, e), with lap-spliced rebars at midspan (f, g) and overview of the FE model of slab GFRP-C2.5 at failure (b).

damage in the rebars and in the rebar-concrete interface. Figure 7(d) illustrates a detail of a rebar in the central part of slab GFRP-C2.5, showing that failure occurred due to tensile rupture of the longitudinal reinforcement (for temperatures well above the T_d). The glass fibres were covered with a black carbon (char) layer; however, in the sections aligned with the main concrete cracks, the fibres had turned into white, indicating the complete decomposition of the resin, including of the carbon black residue layer. Such evidence can be explained by the very wide cracks that developed between the loading

points and across the entire cross section depth, thus exposing the fibres directly to the fire action. The removal of the concrete cover at both extremities of the slabs confirmed that no rebar slippage took place in the anchorage zones, which remained practically undamaged due to the relatively low temperatures measured in those zones (below the T_g at the rebars end). This observation confirmed that the (cold) anchorages were responsible for ensuring the members' load bearing capacity after the rebar-concrete bond had been lost along the length directly exposed to fire, which, as mentioned in the previous section, occurred during an early stage of the tests.

The failure of the slab with lap-spliced reinforcement occurred suddenly, with extensive cracking in the lap splice length (*cf.* Fig. 7(f)). After the concrete cover had been removed, it was possible to observe that failure occurred due to slippage in the lap splice zones (*cf.* Fig. 7g) and that one rebar was broken in the transverse direction, possibly due to the sudden displacement increase at failure. Moreover, it was observed that the surface of the rebars were depleted of the sand coating, resulting from the softening of superficial resin (the maximum temperatures measured were above T_g), and some wrapped fibres also appeared to be broken – this GFRP-concrete debonding failure matches that reported in (Rosa et al. 2019).

5   Conclusions

The experimental and numerical investigations presented in this paper about the fire resistance behaviour of concrete slab strips reinforced with sand-coated GFRP bars allowed drawing the following main conclusions:

- Both experimental and numerical results confirmed that GFRP-RC slabs can attain significant fire resistance (more than 120 min) even if relatively small concrete covers (up to 3.5 cm) are adopted, provided that (i) continuous reinforcement is used, and (ii) the anchorage zones are protected from direct thermal action, by keeping the temperature of the rebars below T_g. Even when temperatures higher than T_d are reached at the bottom reinforcement in the fire-exposed length (causing a complete degradation of the rebar-concrete bond), the load bearing capacity of the member is still ensured by the longitudinal GFRP rebars, which progressively develop a "cable" behaviour, anchored in the cooler extremities of the member – under these conditions, failure occurred due to tensile rupture of bottom reinforcement at the central (*i.e.* heated) zone of the slabs. Moreover, the experimental results showed that the use of the relatively low concrete strength can reduce significantly the fire resistance of slabs – a more extensive concrete cracking of the concrete occurred, causing local heating of the bottom rebars and, therefore, their premature tensile failure.
- Even if the development length recommended in design guidelines is used (for design at ambient temperature), lap splicing can remarkably reduce the fire resistance of GFRP-RC slabs (to less than 30 min) if it is located along the spans exposed to fire. For this reason, splicing should be protected from heat or preferably located over the supports. Additional studies are needed to develop appropriate fire design specifications and detailing provisions in this respect.

- The 3D FE models developed in this paper were able to predict with good accuracy the overall thermal and mechanical responses of the slabs under exposure to fire, including the rebar-concrete bond failure that was observed in the fire resistance tests of the slab with lap-spliced reinforcement – these results also further validate the local bond-slip laws previously (and independently) calibrated by the authors for the GFRP-concrete interface at different elevated temperatures.

References

Nigro E, Bilotta A, Cefarelli G, Manfredi G, Cosenza E (2012) Performance under fire situations of concrete members reinforced with FRP rods: bond models and design nomograms. J Compos Constr 16(4):395–406

Hajiloo H, Green MF, Noël M (2019) GFRP-reinforced concrete slabs: fire resistance and design efficiency. J Compos Constr 23(2):1–13

Carvelli V, Pisani MA, Poggi C (2013) High temperature effects on concrete members reinforced with GFRP rebars. Compos B Eng 54(1):125–132

Nigro E, Cefarelli G, Billota A, Manfredi G, Cosenza E (2011) Fire resistance of concrete slabs reinforced with FRP bars. Part II: experimental results and numerical simulations on the thermal field. Compos Part B 42:1751–1763

Kodur VKR, Bisby LA (2005) Evaluation of fire endurance of concrete slabs reinforced with fiber-reinforced polymer bars. J Struct Eng 131(1):34–43

Adelzadeh M, Hajiloo H, Green MF (2014) Numerical study of FRP reinforced concrete slabs at elevated temperature. Polymers 6:408–422

Rafi MM, Nadjai A (2014) Parametric finite element analysis of FRP reinforced concrete beams in fire and design guidelines. Fire Mater 38:293–311

Kodur VKR, Bisby LA, Foo SH-C (2005) Thermal behavior of fire-exposed concrete slabs reinforced with fiber-reinforced polymer bars. ACI Struct J 102(6):799–807

Rosa IC, Firmo JP, Correia JR, Barros JAO (2019) Bond behaviour of sand coated GFRP bars to concrete at elevated temperature – definition of bond vs. slip relations. Compos B 160:329–340

Bai Y, Vallée T, Keller T (2007) Modeling of thermo-physical properties for FRP composites under elevated and high temperature. Compos Sci Technol 67(15–16):3098–3109

Wang YC, Wong PMH, Kodur VKR (2007) An experimental study of the mechanical properties of FRP and steel reinforcing bars at elevated temperatures. Compos Struct 80:131–140

Hilsdorf H, Brameshuber W (1991) Code-type formulation of fracture mechanics concepts for concrete. Int J Fract 51(1):61–72

Bamonte P, Felicetti R (2012) High-temperature behaviour of concrete in tension. Struct Eng Int 22(4):493–499